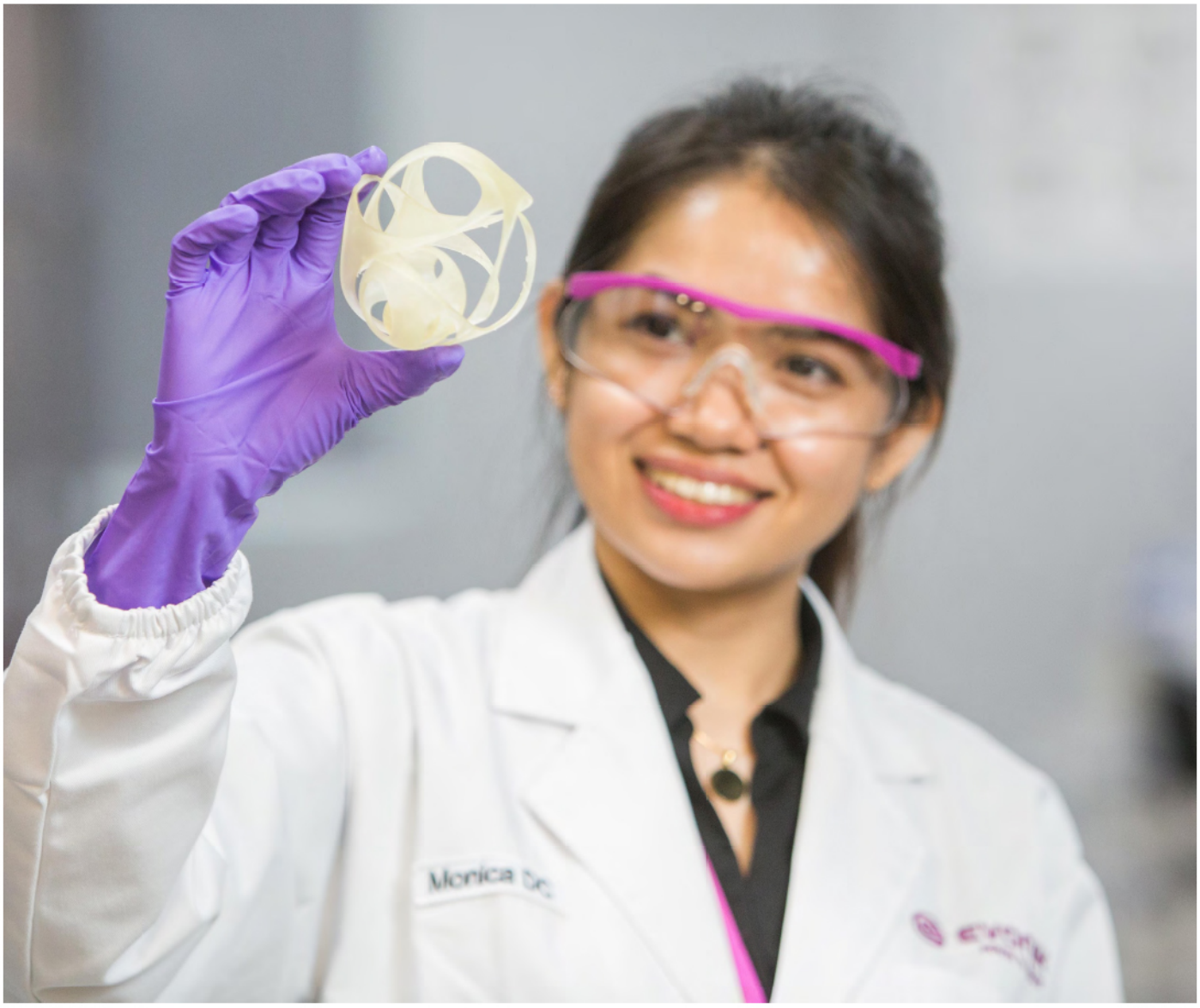

# Pushing the boundaries of chemistry? It takes #HumanChemistry

Make your curiosity and talent as a chemist matter to the world with a specialty chemicals leader. Together, we combine cutting-edge science with engineering expertise to create solutions that answer real-world problems. Find out how our approach to technology creates more opportunities for growth, and see what chemistry can do for you at:

**evonik.com/career**

EVONIK
Leading Beyond Chemistry

Received: 30 April 2021 | Revised: 8 June 2021 | Accepted: 10 June 2021

DOI: 10.1002/pol.20210324

REVIEW

JOURNAL OF POLYMER SCIENCE WILEY

# A practical guide to quartz crystal microbalance with dissipation monitoring of thin polymer films

**Alexandra D. Easley**[1] | **Ting Ma**[2] | **Chikaodinaka I. Eneh**[2] | **Junyeong Yun**[2] | **Ratul M. Thakur**[2] | **Jodie L. Lutkenhaus**[1,2]

[1]Department of Materials Science and Engineering, Texas A&M University, College Station, Texas

[2]Artie McFerrin Department of Chemical Engineering, Texas A&M University, College Station, Texas

**Correspondence**
Jodie L. Lutkenhaus, Artie McFerrin Department of Chemical Engineering, Texas A&M University, College Station, TX 77843, USA.
Email: jodie.lutkenhaus@tamu.edu

**Funding information**
Division of Materials Research, Grant/Award Number: 1905732; Office of Science, Grant/Award Number: DE-SC0014006; National Science Foundation, Grant/Award Number: DGE:1746932

**Abstract**

Quartz crystal microbalance with dissipation (QCM-D) monitoring is a powerful tool used to sensitively examine the real-time responses of polymer films to external responses. For example, the technique is commonly used to monitor film growth, material adsorption, thin film swelling, and ion exchange. With its rapidly expanding use, this review is intended to introduce new users to the basic principles of QCM-D, along with practical challenges and remedies specific to polymer thin films. For both new and experienced users, specific case studies are highlighted including layer-by-layer assembly, electrochemical QCM-D, swelling, sensing, and biological application. Last, the review recommends future directions for research and areas of growth.

**KEYWORDS**

electrochemistry, layer-by-layer assembly, polymer thin film, quartz crystal microbalance with dissipation monitoring, sensing

## 1 | INTRODUCTION

The last 15–20 years have brought enormous growth and development in the application of quartz crystal microbalance with dissipation (QCM-D) monitoring to understand real-time changes in thin films.[1–3] Whereas early publications focused upon method development and data interpretation, the field has shifted toward application. Now, there are many reports of the technique being used as a powerful tool to understand a variety of phenomena including fouling,[4–6] swelling,[7–11] sorption,[12,13] and ion exchange.[14,15] The ability to sensitively monitor mass changes (e.g., 17.7 ng/[cm$^2$·Hz] for a 5 MHz crystal) over small time scales (>100 pts per sec) allows for unprecedented access to mass transport phenomena on a molecular scale.[16]

With many prospective new users, we recognize the need to provide a practical summary of challenges faced in the laboratory setting, especially those encountered in cutting-edge applications. In the first portion of this article, we review the basic principles and operation of QCM-D with special attention to experimental challenges often encountered, but rarely discussed in the literature. For example, bubbles and film delamination are commonly encountered, resulting in data that is unusable and discarded. We present strategies to minimize these challenges, as well as how these intersect with some of the more difficult QCM-D experiments. For example, slow sorption experiments may occur on the same time scale as instrumental drift. In the second portion of this article, we highlight a series of case studies that represent some of the most-active or forward-looking areas to which QCM-D is applied; these include layer-by-layer (LbL) assembly, electrochemical responses of redox polymers, film swelling, gas sensing, and biological applications. It is impossible to examine every aspect of QCM-D monitoring of polymer films, so only selected case studies are presented. The review closes with recommendations and cautions for new users, as well as commentary on application areas of growth.

This review is restricted to the application of QCM-D to polymer films, which present a unique challenge in

  

that they tend to have a viscous component that adds a layer of complexity to viscoelastic modeling of the raw data. To that end, we discuss various models and their appropriate use. Another challenge presented by polymers is their tendency to swell in the contacting media, which can be advantageous (if one is intending to calculate the Flory-Huggins interaction parameter)[9] or disadvantageous (if the polymer dissolves). Other reviews examine porous batteries and supercapacitors electrodes,[17] nanoparticle interactions,[18] and cell behavior on surfaces,[19] to which the reader is referred for a broader view of QCM-D. Many of these reviews examine the case of rigid materials that do not have a remarkable viscous component or do not swell.

## 2 | BASIC PRINCIPLES OF QCM AND QCM-D

### 2.1 | Operating principles

QCM and QCM-D both utilize the converse piezoelectric effect, which results in vibrational oscillations of a quartz crystal when an alternating potential is applied.[20,21] The two methods differ in that QCM-D measures the change in the resonance frequency and dissipation of the oscillations, whereas QCM only measures the change in resonance frequency, Figure 1(A),(B).[18,19,22–27] The changes in frequency and dissipation can be related to the mass associated with the deposited material and its viscoelastic properties. If the deposited material is rigid, there is negligible change in dissipation; however, if the material exhibits a viscous component, then significant changes in dissipation can arise, Figure 1(C). Therefore, QCM can be used to reliably measure homogeneous rigid materials (such as dry polymer films), but when the materials are viscoelastic (such as polymer films in contact with liquid), QCM-D can prove more beneficial.

QCM-D measures both the oscillation frequency and dissipation at multiple overtones, typically 1, 3, 5, 7, 9, 11, and 13, of the resonance frequency.[26] As the overtone number increases, the penetration depth decreases, which allows for insight into certain vertical regions of the adhered film. The penetration depth (δ) of the transverse wave from the oscillation crystal into the coated material and bulk fluid can be calculated for each overtone ($n$) using Equation (1):

$$\delta = \left(\frac{\eta_m}{\pi n f_0 \rho_m}\right)^{\frac{1}{2}}, \quad (1)$$

where $\rho_m$ is the density of the deposited material, $\eta_m$ is the viscosity of the material and $f_0$ is the fundamental frequency of the QCM-D sensor (or 4.95 MHz for the Au coated ≈ 334 μm thick AT-cut quartz crystal). The penetration depth and overtones used for analysis should be considered when determining the optimal coating thickness. For example, in an aqueous solution δ is 240 nm for $f_0$ and 68 nm for the 13th overtone.[28] Several reports nicely visualize the penetration depth for each overtone.[17,29,30]

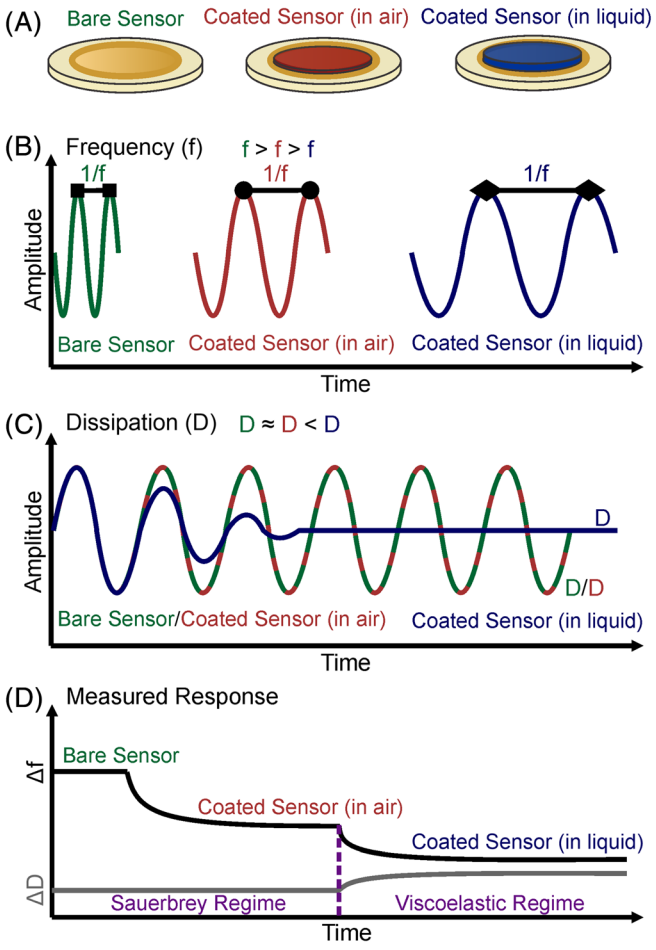


**FIGURE 1** (A) Depictions of a bare QCM-D sensor, a thin polymer film-coated sensor in air, and a swollen polymer film-coated sensor in liquid. (B and C) Qualitative frequency and dissipation changes in sensor oscillations, respectively, due to the polymer coating in air and in liquid. (D) A mock QCM-D response for the change in a single frequency overtone (Δf) and dissipation (ΔD) as the sensor is first coated with polymer and then swollen in liquid with the Sauerbrey and viscoelastic model regimes identified. Decreased frequency is associated with increased mass of the coated sensor, and increased dissipation is associated with softening of the film

### 2.2 | Modeling of the QCM-D response

Perhaps one of largest challenges for new users is the selection of the proper model. There are four prevailing

models used for describing QCM-D data in the literature: the Sauerbrey model, the viscoelastic models (Voigt and extended Voigt), and the hydrodynamic model.[17,18,20,30,31] Of these, the Sauerbrey and Voigt models are most commonly invoked for polymer films. The Maxwell model has also been considered but is not as common.[25,32] (Figure 2)

### 2.2.1 | Sauerbrey model

The Sauerbrey model (Equation (2)) states that the change in mass of the adhered material (Δm) is proportional to the change in frequency (Δf):[17,33]

$$\Delta m = -C\frac{\Delta f}{n}, \tag{2}$$

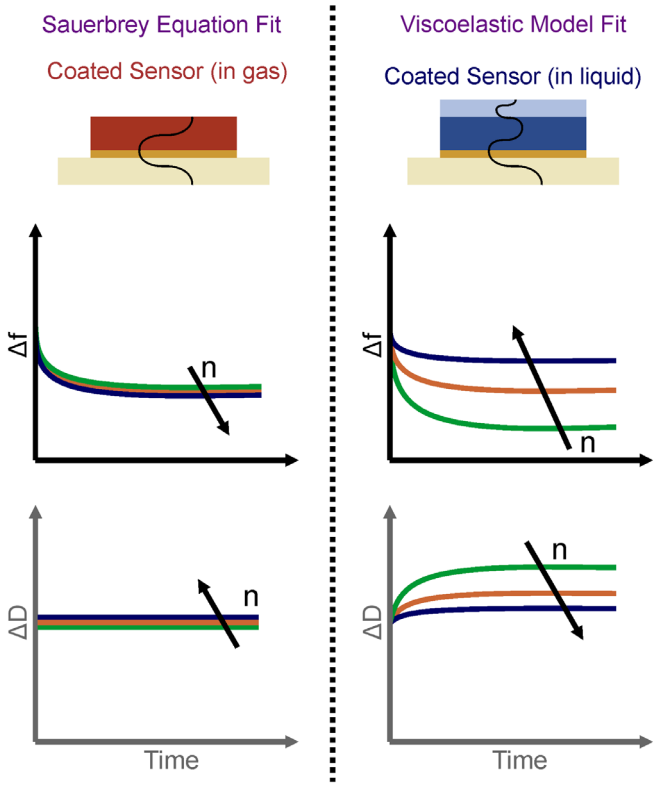


**FIGURE 2** The overtone trends for frequency and dissipation for data that could be fit with the Sauerbrey equation or a viscoelastic model. (top) The black line through the sensor and film represents the oscillation of sensor, where there is slight frequency change (but no change in dissipation) for the polymer film in gas, whereas there is both a frequency and dissipation change for the polymer film in liquid. (bottom) Rigid films that do not display strong differences among overtones in frequency or dissipation can be fit with a Sauerbrey model; films with a viscous component may show varying frequency or dissipation responses with regard to overtone

where $C$ is the mass sensitivity constant of the sensor. This model is used to fit data for QCM-D (or QCM) when there is no change in dissipation and is suitable for uniform and rigid materials. Examples of such materials include glassy polymers in air or metallic coatings in air/liquid.[34–36] The Sauerbrey model may be used for a polymer coating in contact with liquid if the change in dissipation is small ($\Delta D \approx 0$). Reviakine et al. suggested that $|\Delta D_n/(\Delta f_n/n)| < < 4 \times 10^{-7}$ Hz$^{-1}$ indicates that the Sauerbrey equation may be used.[31] Elsewhere, Cho et al. suggested that $|\Delta D_n/\Delta f_n| > 1 \times 10^{-8}$ Hz$^{-1}$ implies that viscoelastic models should be used.[37] These values arise from considering the ratio of ΔD and Δf obtained as a solution to the viscoelastic wave equation ($\Delta D_1/\Delta f_1 \approx 2/f_0 \approx 4 \times 10^{-7}$ Hz$^{-1}$) when the film becomes thick and viscoelastic.[27]

### 2.2.2 | Viscoelastic models

The Voigt or the Kelvin-Voigt viscoelastic models relate the measured dissipation factor ($D$), shown in Equation (3), which is dependent on the deposited material and the measurement environment (air/liquid).

$$D \approx \frac{E_{\text{dissipated}}}{E_{\text{stored}}} \tag{3}$$

In this model, frequency and dissipation are functions of the deposited material's thickness ($d_m$), density ($\rho_m$), viscosity ($\eta_m$), and shear modulus ($\mu_m$), as well as the density ($\rho_b$) and viscosity ($\eta_b$) of the bulk contacting liquid or gas.[27,34] Experimentally, the most common way for instruments to determine the dissipation factor is the "ring-down" method, which has been described in detail elsewhere.[31,38] The equations relating the frequency and dissipation to the above parameters can be found in previous review papers.[18,25,30,36] This model should be used to describe data if the material is homogenous and if distinct dissipation changes are observed ($\Delta D > 0$). Also, this model assumes "no-slip" boundary conditions and calculates the change in mass using film thickness ($d_m$) and $\rho_m$.[27] If the polymer film is sufficiently thin ($d_m/\delta < < \sqrt{\chi/2}$ for $\chi > 1$ or $< < 1-\chi/2$ for $\chi < 1$, where $\chi$ is the viscoelastic ratio or the ratio between the storage and loss moduli), then the Sauerbrey equation is recovered (Equation (2)).[27] Multiple overtones (excluding the first overtone or fundamental frequency) should be utilized to achieve a quality fit; a minimum of three overtones are required, but more could be used for greater accuracy.[39–41] Examples of materials that can be described using the viscoelastic Voigt model are polymers swollen with solvent and polymers above the $T_g$.[34,39,42]

The extended Voigt model is an expansion of the viscoelastic Voigt model described above, with the provision that the viscosity and complex shear modulus, $G^*$, of the deposited film are frequency dependent, as shown in Equations (4) and (5):[30,43–45]

$$G''(f) = 2\pi f \eta(f), \tag{4}$$

$$G^* = G' + iG'', \tag{5}$$

where $G'$ is the storage modulus, and $G''$ is the loss modulus. The frequency dependence of $G'$ and $G''$ can follow a linear relationship or power law, with power laws using exponents $\alpha'$ and $\alpha''$ being more common.[43–45] The extended Voigt model should be considered if the coated material is a two-component system where effective film properties are used, such as polyelectrolyte multilayers (PEMs), or if a material exhibits a frequency-dependent modulus.[44,46] Another indication for this model is when the adhered polymer exhibits a viscoelastic relaxation in the frequency range considered by the QCM-D instrument ($\approx$ 5 MHz for the fundamental frequency to $\approx$ 65 MHz for the 13th overtone).[47]

### 2.2.3 | Hydrodynamic model

The hydrodynamic model accounts for frequency shifts that are dependent on penetration depth (i.e., different overtones will exhibit different shifts in frequency), which is appropriate for porous or particulate films in contact with a liquid.[31,48–50] This model accounts for liquid that is trapped or entrained in the porous/particle coating. This model is less common for polymer films, but more popularly used to describe electrodes or polymer particles.[17,30,51] This model can be used to estimate the particle radius (r), the inter-particle distance (L), and the particle surface fraction (φ). For solving this model, a complimentary characterization technique such as dynamic light scattering (DLS) or atomic force microscopy (AFM) should be used to confirm particle/surface morphology. This model is not currently included in most commercial fitting software and must be applied by the user.

### 2.2.4 | Challenges associated with applying models

An important consideration when analyzing and reporting QCM-D data is the error associated with film properties obtained from the fitted model. For example, Johannsmann demonstrated that a difference of 25% can occur when determining thickness from raw data when the viscoelastic constants are varied.[52] In other work, Johannsmann reported an error of approximately 10% for viscosity measurements.[47] Sandman et al. showed that the viscoelastic properties of polymer films can be measured most accurately for film's with a ratio of thickness ($d_m$) to shear wavelength of mechanical oscillation ($\lambda_n$) between 0.05 and 0.20.[45] As a demonstration of fitting error, Sandman et al. also showed that the viscoelastic Voigt model provided fit values (such as modulus) even in the Sauerbrey regime where no viscoelastic behavior was observed.[45] Our group has found variations in mass changes determined from the viscoelastic Voigt model when using density approximations for films that are assumed to be homogenous, but may have heterogeneous sections.

## 2.3 | QCM-D sensors and depositing the polymer of interest

Many sensors are available that allow for a wide variety of QCM-D applications. The most common sensors used in literature are gold- (Au) and silicon dioxide- ($SiO_2$) coated 5 Hz quartz sensors. When selecting a sensor, the stability in the conditions of interest and surface charge are important considerations. For example, Wang et al. show that polyelectrolyte deposition can vary with sensor type (Au, $SiO_2$, $Al_2O_3$, or Ti) due to surface differences.[40]

Regardless of the sensors used, they should be cleaned before use to ensure that the sensor quality is high. The cleaning protocol is sensor-specific and should be identified before any experiment is carried out.[53] For Au-coated sensors, our typical cleaning procedure is: 10 min UV/ozone treatment, immersion in a cleaning solution (5: 1: 1 ultrapure water: ammonia [25%]: hydrogen peroxide [30%]), rinsing with ultrapure water, drying with $N_2$ gas, and finally 10 min UV/ozone treatment. Failure to properly clean a sensor can lead to loss of the fundamental frequency and poor model fitting.

For QCM-D measurements, a homogenous thin film of polymer is required to collect high-quality data and for meeting the assumptions of the fitting models. The most common techniques used to deposit polymers on a QCM-D crystals are drop casting,[54] spin-coating,[34,55,56] spray-coating,[49,57] electrodeposition,[58] and flow deposition.[13,14,59–62] We first discuss ex situ coating of the crystal. Drop casting is one of the simplest methods of thin film fabrication, where a small amount of polymer solution is deposited onto the surface of the QCM-D sensor, leaving behind a thin polymer film after evaporation. However, this method can lead to irregular films and

have reproducibility issues. For the case of spin-coating, a polymer solution is deposited onto the sensor of interest, which is then rotated at high speed to evenly spread the solution across the surface. As the solution spreads, the solvent evaporates leading to a homogenous thin polymer film. Spin-coating is advantageous because it typically results in a uniform, thin film with an optimal thickness for QCM-D. However, one disadvantage of spin-coating is that excess material is irrecoverably lost to the process, which may be undesirable for expensive or valuable materials. Spray-coating aerosolizes a polymer solution for deposition onto the sensor's surface, followed by solvent evaporation resulting in a homogenous thin polymer film. The advantages of this method are the simple coating of multiple QCM-D crystals at one time and the favorability for polymer particle deposition to prevent aggregation. However, this method—as with spin-coating—leads to the high loss of material. In all of these ex situ coating approaches, the excess film (not on the active sensor surface) must be removed or else its presence will influence the QCM-D response.

The two most common in situ polymer depositions methods are electrodeposition and flow deposition (or sequential flow deposition). For these methods, the baseline QCM-D data is collected on a bare sensor followed by polymer deposition within the QCM-D module itself. These methods allow the frequency and dissipation (or mass/thickness after fitting) to be measured throughout the deposition process. This also allows one to control deposition to achieve an appropriate thickness. Electrodeposition typically utilizes an electrochemistry QCM-D (EQCM-D) module, which allows for the application of current or voltage during collection of QCM-D data. For electrodeposition, a solution of monomer and supporting electrolyte are flowed into the EQCM-D cell. After the cell is filled, a current or voltage is applied which results in electropolymerization on the surface of the QCM-D sensor. This method is advantageous for quick and reliable fabrication of a thin polymer films, such as polypyrrole.[58] However, one disadvantage is that this process is limited to monomers that can be polymerized electrochemically or charged polymers in contact with a QCM-D sensor with a metallic surface, such as Au.

Flow deposition is a very common in situ method and is typically utilized for sequential deposition of charged polymers (such as LbL assembly).[13,14,59–62] In this method a polymer solution, usually of opposite charge relative to the sensor's surface layer, is flowed through the QCM-D cell, and the polymer adsorbs to the surface. This is then repeated while alternating the charge of the polymer being flowed and typically includes rinse stages to remove any non-adhered polymer. However, this method can be time-intensive and does require a significant excess of polymer solution to conduct the flow process.

## 3 | PRACTICAL EXPERIMENTAL CHALLENGES

With QCM-D being a sensitive technique, many practical experimental challenges can be encountered during one's experiment that are not often discussed within the literature. We examine here several challenges that we have faced, including finding the proper film thickness, delamination and dissolution, bubble formation, and instrumental drift.

### 3.1 | Using an appropriate film thickness

Depending on the fundamental frequency of the sensor used, QCM-D measurements can be as sensitive to as low as 4.4 ng/(cm$^2$·Hz). The higher the fundamental frequency, the better the sensitivity of the sensor. Depending on the viscoelastic nature of the film, it has been recommended to maintain a film thickness in the approximate range of 1 Å–1 μm.[63] In-house experiences have indicated that about halfway through this range, the signal-to-noise ratio of the 13th overtone gradually reduces and eventually leads to the loss of signal. Further increases in thickness lead to the loss of the 11th overtone and so on. In terms of mass, another researcher has reported the upper limit to be roughly 96 μg/cm$^2$.[64] Also, operating within the acceptable thickness range is important because many films are subject to swelling if a liquid environment is to be employed.[65] Among the previously discussed ex situ techniques, spin-coating is most commonly used to obtain thin and uniform films (<150 nm without annealing) and provides precise control over film thickness.

### 3.2 | Delamination and dissolution

During QCM-D monitoring, delamination and dissolution of the original polymer film can hinder interpretation of the results. Delamination often occurs due to mechanical mismatch between the polymer film and the quartz crystal caused by large changes in the external environment, such as humidity, temperature, and pH. Past work has observed delamination in the case of a poly(3,4-ethylenedioxythiophene) derivative, PEDOT-S:

H.[55] Delamination is almost always undesirable because it prevents further data acquisition.

On the other hand, dissolution is exemplified by the molecular loss of polymer or material from the film into the external contacting solution. Both delamination and dissolution phenomena lead to a decrease in the mass of the polymer film, indicated by an increase in frequency during the process, Figure 3(A). In comparison, dissolution usually happens more gradually than delamination and can be monitored over the course of the experiment. Past work has observed dissolution in case of poly(methyl adamantyl methacrylate-co-methacrylic acid),[66] poly(N-isopropylacrylamide),[67] and sulfonated polystyrene-block-poly(ethylene-ran-butylene)-block-polystyrene.[68] As shown in Figure 3(B), Persson et al. reported that swelling and dissolving phenomena occur depending on the concentration of PEDOT-S:H, a water soluble polymer, in aqueous electrolyte; they further observed through QCM-D that cracking and detachment occurred sequentially by the electrochemical oxidation process.

## 3.3 | Bubble formation

When working in the liquid phase, the presence of gas phase bubbles flowing through or forming during the flow may attenuate the system and lead to a short-circuit in which the overtone signals are lost, Figure 4.[2] A common cause for bubble formation is differences in temperature between the chamber and the ambient conditions.[16,69] When the chamber temperature is set significantly below or above room temperature while flow is set at a constant rate, the chances of bubble formation increase. Our in-house experience indicates that chamber temperatures as low as 40–50°C can result in undesirable bubble formation if the flow solution is at room temperature. One simple answer is to reverse the flow of fluid until the bubble is eliminated. However, this clearly does not solve the root-cause of the problem. A more effective answer involves equilibrating the flow solution to the intended chamber temperature prior to the experiment, thus eliminating the temperature difference. Another resolution is to degas the solution prior to flow.[24,70] Asides from

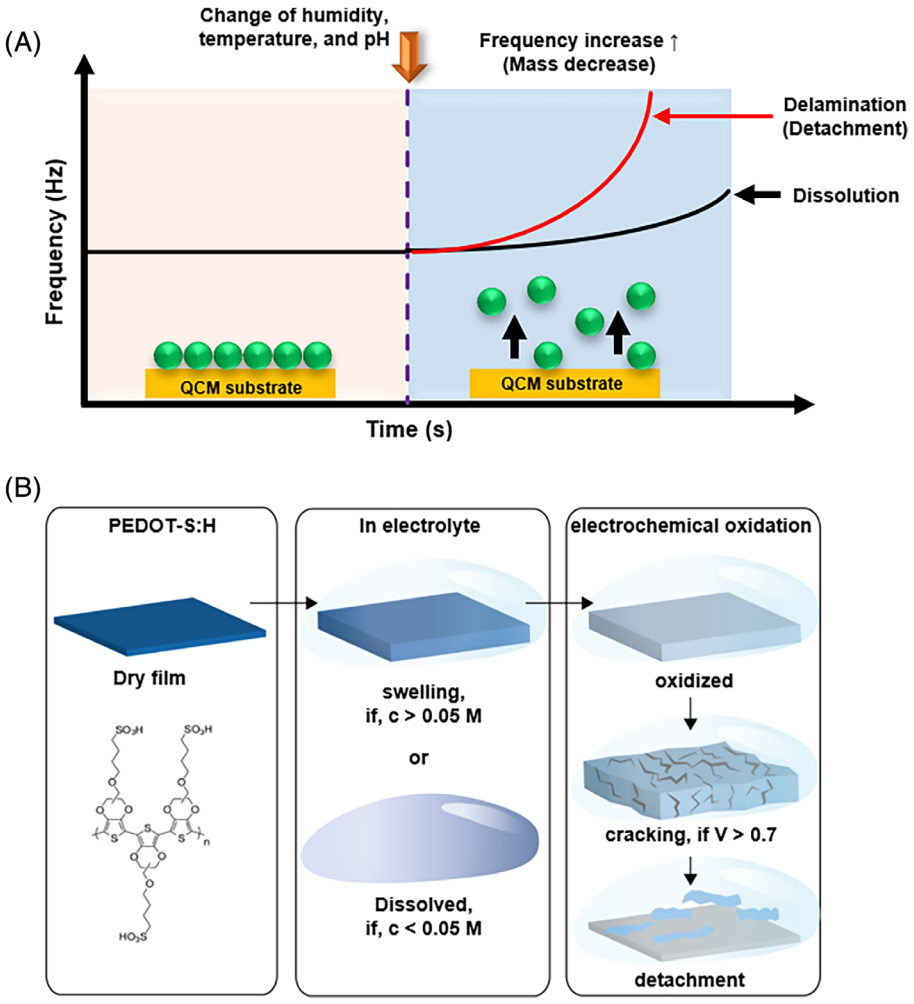


FIGURE 3 (A) Schematic illustration of detachment (delamination and dissolution) and subsequent QCM-D response. (B) When a thin film of PEDOT-S:H (left panel) is submerged in aqueous electrolyte (middle panel), and is electrochemically oxidized in an aqueous electrolyte (right panel).[55] Adapted with permission[55] copyright 2014 American Chemical Society

the flow of bubbles through the system, it is also possible to have smaller bubbles deposited on the sensor itself.[70] Lastly, in more complex systems with buffer flow, air bubbles may be eliminated through a buffer flush valve.

### 3.4 | Instrumental drift versus phenomenological response

Frequency drift is regularly encountered in QCM-D experiments, so it is important to distinguish drift versus true experimental responses. A baseline is necessary for all experiments because it helps distinguish the quality of the crystal as well as the frequency drift. We normally examine the baseline response of the bare crystal in air and in the intended liquid medium, as well as the coated crystal in the same. Once a baseline is established and the drift is acceptable, then the experiment may proceed as planned. For a QSense E4 model, Biolin Scientific suggests that "normally, a clean 5 MHz sensor crystal operated at 25.00 ± 0.01°C should drift < 0.5 Hz/h (<1.5 Hz/h) in the frequency values and $<2 \times 10^{-8}$/h ($<2 \times 10^{-7}$/h) in the dissipation values in air (water)" when considering the third overtone (or 15 MHz harmonic), as seen in Figure 5(A). Accordingly, any response greater in magnitude than the drift can be assigned to that of the coated material. Figure 5(B) shows a hypothetical case in which a coated material is used in the context of a gas-sensing experiment; a small magnitude response may compete with drift, so the two must be compared. Figure 5(C) shows a hypothetical case in which a polymer swells upon exposure to a swelling agent; in this case a slow response may compete with drift, especially over longer times.[9] In the latter case, many authors will select a consistent time to mark the swollen thickness instead of waiting for the long swelling equilibration period.

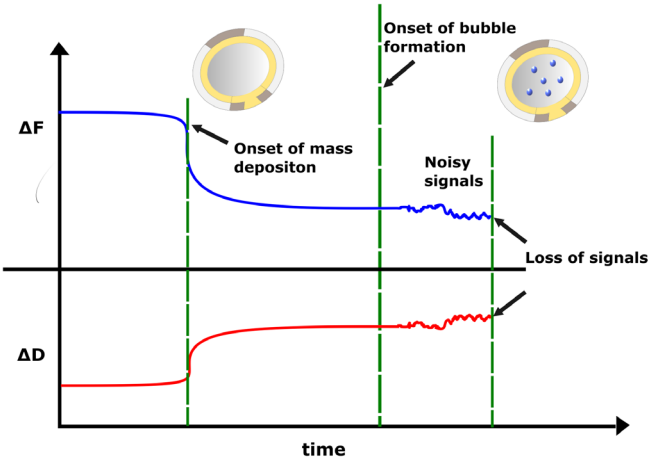


FIGURE 4 Bubble formation during QCM-D measurements leads to noisy signals and an imminent loss of overtone signals

## 4 | SPECIFIC CASE STUDIES

Having addressed the more technical aspects of QCM-D of polymer coatings, we next turn to specific case studies in which we highlight the differences in QCM-D

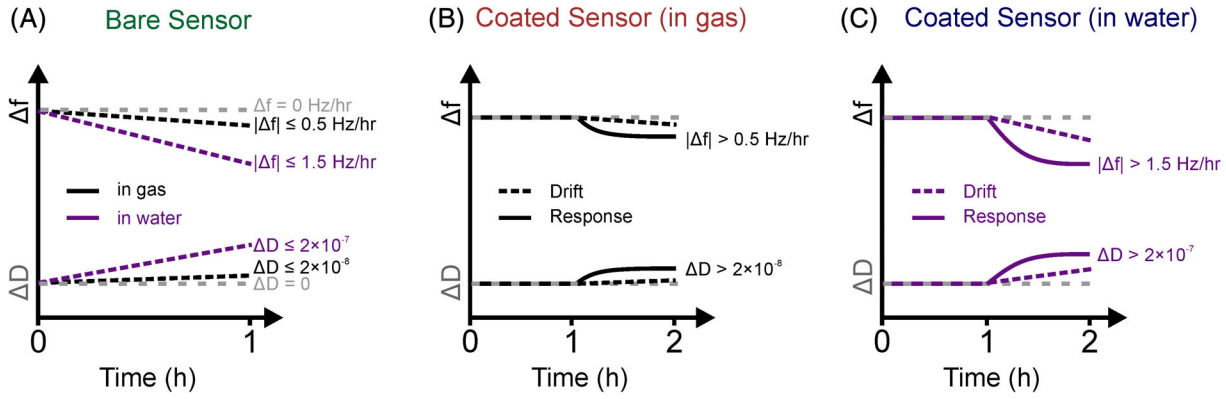


FIGURE 5 The QCM-D response for: (A) signal drift of a bare sensor in a gas (black line) and water (purple line) compared to no response (gray), (B) gas absorption (low ppm) by a polymer-coated sensor with small magnitude changes, and (C) swelling of a polymer-coated sensor in water or solvent with larger magnitude changes and slow response time. The labels in each figure denote the recommended acceptable signal drift. If the magnitude is larger than those denoted, it is typically considered an experimental response. The gray dashed line denotes the case of no drift, and the black and purple dashed lines denote the cases of drift in air and liquid, respectively. The solid lines signify hypothetical experimental responses in which the signal is larger than the drift

operation and data interpretation from scenario to scenario. LbL assemblies, redox-active polymers, polymer sensors, and biomolecule sorption are selected as case studies. Rather than perform an exhaustive literature review of each scenario, we focus upon a few select reports in depth for the benefit of future users.

## 4.1 | LbL assemblies

QCM-D has been popularly used both to monitor the build-up and response of multilayer polymer films prepared using the LbL assembly technique.[12–15,19,71] In this section, we discuss the various applications of QCM-D to multilayer films, and we present two case studies in deeper detail.

The QCM-D instrument and chamber may be used to monitor the LbL process in situ by the alternate deposition of oppositely charged polyelectrolytes.[13,14,59–62] For example, QCM-D has been used to monitor the effect of the polymer solution concentration, ionic strength, or pH on multilayer growth.[61,62] Between each polyelectrolyte layer deposition, a rinse step is typically added to eliminate excess charge adsorbed from the previous layer and promote the formation of a more uniform layer. To build a polyelectrolyte multilayer (PEM), these deposition and rinse steps are repeated until the desired number of layers is obtained. In order to monitor film build-up, the multilayer is formed within the QCM-D flow module by physically switching the chamber inlet tubing from solution to solution. One challenge that we have encountered is that the LbL film builds up on the interior of the chamber and tubing over time. Therefore, after each experiment, it is advisable to flow sodium dodecyl sulfate (SDS) followed by deionized water through the flow module to prevent this build-up.

Post-assembly, the response of the multilayer to changes in the external media such as temperature, humidity, pH, or ionic strength[12–15] has been of interest. Such changes cause the multilayer to swell, contract, or dissolve, manifesting as changes in hydrated mass, thickness, or viscoelasticity. When a variety of solutions are used as external media (to affect changes in the multilayer) within a single study, it becomes necessary to breakdown the entire data set into various periods corresponding to each fluid used and indicate the fluid properties before applying a model.[27] For example, challenges may arise in cases where two successive solutions are largely different from each other, as in the case of having very different ionic strengths.

For the first case study, we have chosen a research work that highlights three possible events of mass adsorption, desorption, and no deposition during LbL assembly. Vander Straeten and Dupont-Gillain[72–74] applied QCM-D monitoring to define a self-assembly technique involving a templating agent to obtain

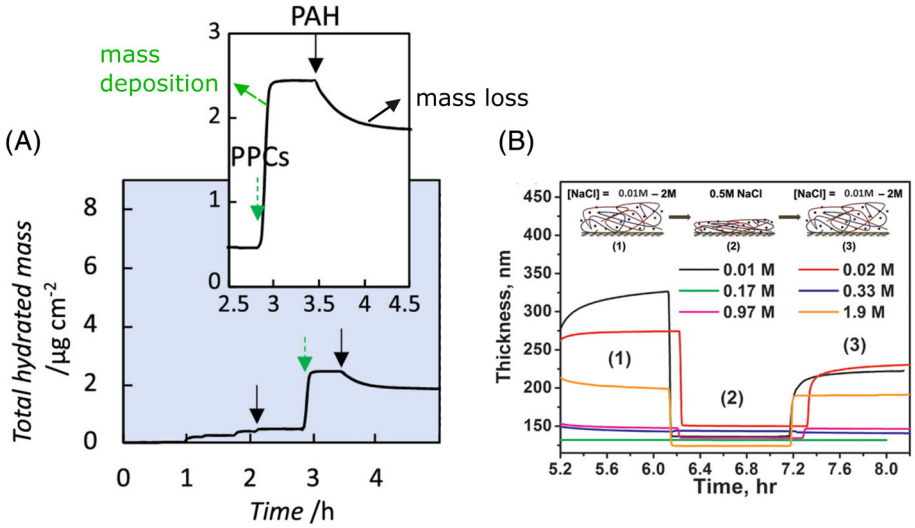


FIGURE 6 (A) LbL deposition of PAH/PPC multilayers showing occasions of mass deposition upon addition of PPC (green arrows) and mass loss upon addition of PAH (black arrows). Adapted with permission from ref. 72, copyright (2020). (B) Swelling and deswelling of PDADMA/PSS films as the overlying solution is switched between 0.01 and 2 M NaCl solution (steps 1 and 3 at matching NaCl concentration) and 0.5 M NaCl solution (step 2). Reprinted with permission from ref. 15, copyright (2016). LbL, layer-by-layer; PAH, poly(allylamine hydrochloride); PPC, protein-polyelectrolyte complexes; PDADMA, poly(diallydimethylammonium); PSS, polystyrene sulfonate

hydrated PEM films. Protein-polyelectrolyte complexes (PPCs) of tunable charge (positive or negative) were prepared from lysozyme (Lys) (protein) and polystyrene sulfonate (PSS) (polyelectrolyte). The PPC was then LbL-deposited alternately with poly(allylamine hydrochloride) (PAH). Two layer pairs of PAH/PSS were first deposited as an anchor layer and to minimize the effects of the sensor. Following this, five layer pairs $(PAH/PPC)_5$ were prepared and for comparison $(PAH/Lys)_5$, $(Lys/PSS)_5$, and $(PAH/PSS)_5$. From observation, all systems demonstrated three possible outcomes in the QCM-D mass data evident in Figure 6(A). (1) No mass change: This demonstrated unsuccessful LbL assembly, arising from the combination of a positively charged PPC and positively charged PAH. The lack of electrostatic attraction hindered assembly; thus, no frequency change was observed. (2) Mass increase: This demonstrated a successful layer deposition, arising from sufficient electrostatic attraction. This was evident in all layers in $(Lys/PSS)_5$, $(PAH/PSS)_5$, and $(PAH/PPC)_5$ samples (for which PPC was negatively charged). (3) Mass decrease: This demonstrated a loss of mass from the existing film on the sensor and was evident in the PAH deposition step in the $(PAH/PPC)_5$ samples. It was suggested that highly positive PAH adsorbed into the PPC, which caused the release of Lys from the multilayer.

In our own work, we have studied the influences of hydration, ionic strength, pH, and temperature on poly(diallydimethylammonium) (PDADMA)/PSS and PAH/poly(acrylic acid) (PAA) multilayers. Using a temperature-controlled QCM-D, the glass transition of hydrated PEMs at various ionic strengths and pH values was examined.[61,62] In other works, we have studied the effect of salt concentration on the swelling properties of both PEMs as shown in Figure 6(B).[14,15]

Here, we elaborate upon our study of the swelling of PDADMA/PSS multilayers (prepared in 0.5 M NaCl) in response to KBr, NaCl, NaBr, and KCl aqueous solutions.[14] The goal of this study was to provide a better understanding of ion exchange between monovalent salts and multilayer counter ions. Four swelling-regimes were identified depending on the salt concentration. At lower salt concentrations (0–0.001 M KBr), the multilayers expanded largely as a result of electrostatic repulsion. Between 0.01 and 0.5 M KBr, the multilayers slightly contracted as a result of a sufficient amount of charge compensation within the PEM. At concentrations higher than the assembly concentration and between the critical salt concentration (0.5–1.6 M KBr), the films swelled as a result of the disruption of polycation-polyanion ion pairs. At 1.6 M KBr, a critical salt concentration was reached, and the multilayer deconstructed due to excessive charge screening. Comparison among other monovalent salts showed that both NaCl and KCl produced a similar swelling trend (19% and 22% swelling respectively at 1.6 M) and equally NaBr and KBr (93% and 98% swelling respectively at 1.6 M). This showed that the largest ion exchange occurs for the $Br^-$ ion, whereas exchange was relatively lower for $Na^+$, $K^+$, and $Cl^-$.

## 4.2 | Electrochemical QCM-D of redox polymers

When combined with electrochemistry, QCM-D can provide information on mass and structural changes associated with electron transfer processes occurring within an electrode. Electrochemical QCM-D (EQCM-D) has been successfully used to characterize rough/porous inorganic electrode materials for energy storage and conversion.[49] The technique has also been widely used to analyze the formation, growth, and mechanical properties of solid electrolyte interphase (SEI) films under various conditions.[75,76] These studies have been thoroughly reviewed elsewhere.[17,30,77] Here, we specifically focus on the application of EQCM-D to redox polymers, with special attention to the practicality of obtaining data of the highest quality.

A typical aqueous electrochemical QCM-D (EQCM-D) module consists of a three-electrode configuration, where the quartz crystal sensor surface acts as the working electrode, a Pt plate is the counter electrode, and a customized low-leak Ag/AgCl electrode is used as the reference electrode, Figure 7. The Pt counter electrode, which also acts as the top wall of the module, reduces the volume above the sensor to about 100 μl. For nonaqueous cells, other reference electrodes (e.g., silver wire quasi-reference electrode [QRE], lithium ribbon) have been utilized. Also, nonaqueous cells require solvent-resistant fittings, such as Viton O-rings and Teflon flow channels. If desired, the module can be used in a two-electrode configuration by sealing off the reference electrode port. Three of the ports shown in Figure 7 are used as feedthroughs for the potentiostat. The other two ports are connected to inlet and outlet tubing, and experiments can be operated in either flow or static modes.

For polymer films, EQCM-D applications have included monitoring the evolution of the viscoelastic properties and swelling characteristics,[11,78,79] quantifying ion/solvent transport, and ionic-to-electronic coupling efficiency.[65] Besides, EQCM-D has also been applied to characterize and optimize electropolymerization/deposition of conjugated polymers.[80] In the area of biosensors, where biomolecules adsorb onto the surface, EQCM-D has been utilized while biasing the surface to monitor the biomolecular response of redox proteins, cells, DNA, and

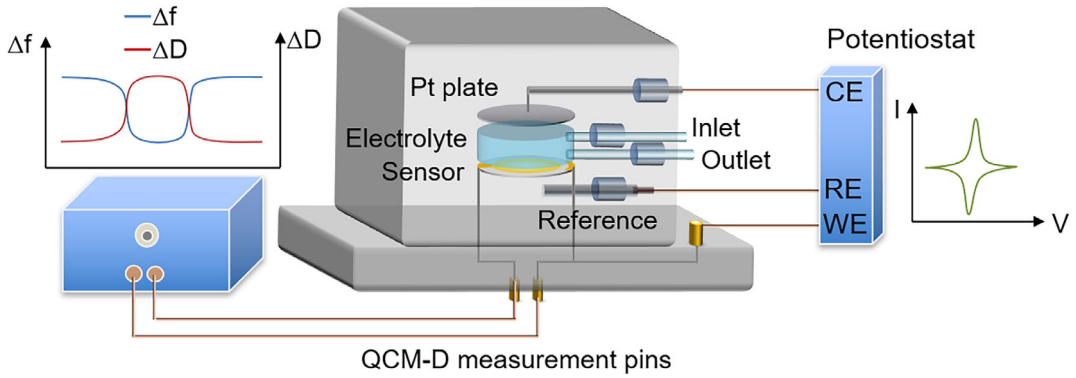


**FIGURE 7** Schematic diagram of the EQCM-D set-up. The sensor mounted at the bottom serves as the working electrode; any changes happening at the surface in the electrochemical environment are measured in real time by monitoring the frequency (f) and dissipation (D) changes of the sensor crystal using QCM-D. The Pt ceiling acts as the counter electrode, and the reference electrode is mounted in the outlet flow close (~4–5 mm) to the working electrode

other species.[81] Cyclic voltammetry is a common electrochemical method combined with EQCM-D to quantify changes in mass and viscoelasticity during the oxidation and reduction processes of the adhered redox polymer.[82] Specifically, the current is recorded along with changes in frequency and dissipation in response to a linear voltage sweep. A typical EQCM-D experiment begins with taking baseline measurements of the bare sensor in both air as well in the electrolyte, followed by similar baseline measurements of the coated sensor to determine the dry coating's thickness. Next, the electrolyte is pumped into the chamber with the coated sensor, and then the cell is kept for some time (>15 min) to equilibrate with the electrolyte. Because this is not fully sufficient to equilibrate the polymer, additional conditioning via repeated electrochemical cycling is often preferred. The number of conditioning cycles varies for each redox-active polymer depending upon the competing factors of polymer dissolution and electrolyte penetration. After conditioning, the intended cyclic voltammetry studies at varying scan rates can commence simultaneously with QCM-D.

With the raw data in hand, the user then must analyze how frequency, dissipation, and charge transferred ($Q$) are coupled. This requires the calculation of $Q$, which is obtained by the integration of the current passed with respect to time. However, the charge transfer calculation methodology differs from researcher to researcher. The CV is split into oxidation and reduction cycles, but different researchers have applied different baseline methodologies to correct the current (thus affecting the value of $Q$). In one case, a tangent line from the initial halfwave sweep was simply taken as the baseline correction.[83] In another case, no baseline at all was applied.[34] More recently, we have adopted an equal area baseline correction in that a baseline is drawn such that $Q_{red}$ is forced to equal $Q_{ox}$. We have found good results and consistency with this method, but the disadvantage is that it implicitly assumes a Coulombic efficiency of 100%. Additionally, using equal area baseline accounts for any non-Faradaic processes that may occur, whereas the tangent methodology does not. Using the data from QCM-D, mass versus time can be obtained and compared to the corresponding plot of $Q$ versus time. Combining the plots together allows one to visualize mass versus $Q$ to obtain greater insight toward the coupled electron-ion transport mechanism. The slope of mass versus $Q$ may be used to calculate the number of cations/anions transporting during the redox reaction. In the case where the transporting mass is greater than predicted, then the mass difference may be used to calculate the number of solvent molecules accompanying the cation or anion. If electrolysis of the solvent is a concern, a blank cell should be examined in analogous conditions to quantify any resulting current and to correct $Q$. The apparent molecular weight of the transporting species can be calculated using Equation (6), and the number of solvent molecules accompanying the ion can be calculated using Equation (7).

$$\frac{\Delta m}{\Delta Q} = \frac{M_w^{app}}{nF}, \tag{6}$$

$$\frac{\Delta mnF}{\Delta Q} - M_w^{anion} = \text{no. of solvent molecule} \times M_w^{solvent}. \tag{7}$$

A case study of the cyclic voltammetry/EQCM-D response of a representative redox-active polymer is presented here, in which the redox mechanism of poly(2,2,6,6-tetramethylpiperidinyloxy-4-yl) (PTMA) and

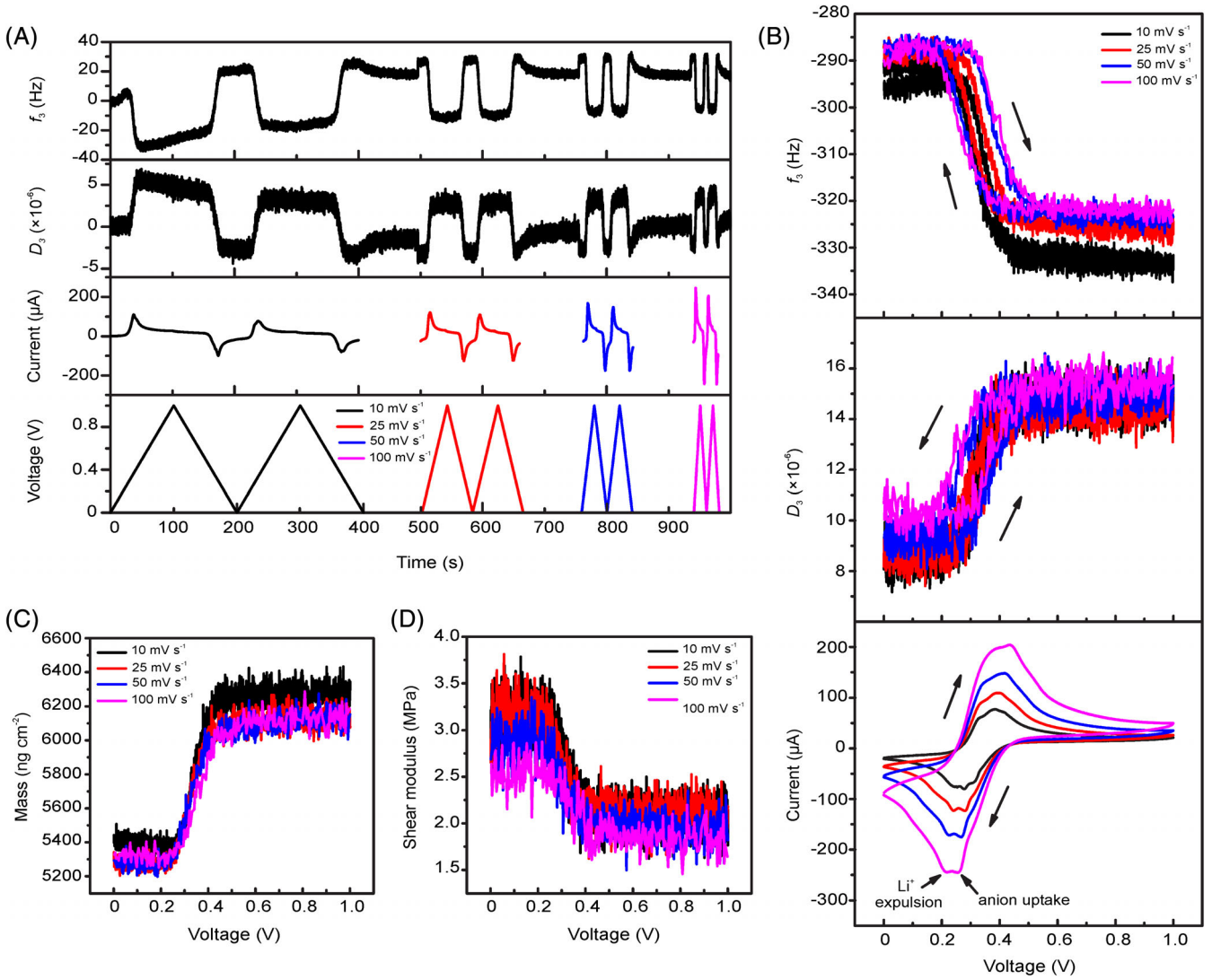


**FIGURE 8** Comparison of in situ EQCM-D and cyclic voltammetry of PTMA for varying scan rates. (A) Frequency ($f_3$) and dissipation ($D_3$) responses of the third overtone with respect time. Two cycles at each scan rate were performed, followed by equilibration in the liquid electrolyte for 100 s. (B) Frequency ($f_3$) and dissipation ($D_3$) responses of the third overtone with respect to voltage. (C) Mass and (D) shear modulus profiles of a PTMA cathode during oxidation at all scan rates obtained from applying a Voigt model to the EQCM-D data. The working electrode was PTMA, and the electrolyte was 0.5 M $LiCF_3SO_3$ in propylene carbonate (PC). Pt plate was the counter electrode. The potential window was 0–1 V versus silver wire quasi-reference electrode (QRE). Adapted with permission from ref. 34. Copyright 2019, nature group journals

its coupled ion/solvent transport was considered by us.[34] PTMA was coated onto a Au-coated quartz crystal and the response was measured during cyclic voltammetry for varying scan rates, Figure 8. The QCM-D response tracked well with cyclic voltammetry and was reversible, indicating that the mass and viscoelastic property changes were recoverable. The change of mass and shear modulus were obtained from viscoelastic modeling of the raw data using the Voigt model, leading to a quantitative view of mass transport associated with the doping process. Upon oxidation, PTMA converts to an oxoammonium cation form and an anion dopes the site. This is exemplified by the decrease in frequency (Figure 8 (B), top) and the increase in mass (Figure 8(C)) at higher voltages. Upon reduction, the reverse process occurs. With closer inspection of the response, the real-time mass transfer of anions, lithium cations, and solvent molecules during the reduction and oxidation of PTMA was quantified, which allowed for the resolution of lithium expulsion and anion uptake in the organic radical polymer. Finally, we presented an analysis method for PTMA by which the mass exchanged per electron transferred was quantified, and, in some cases, the number of solvent molecules transferred could be calculated (ranging from

0.3 to 3.2 solvent molecules based on different scan rate). In subsequent work, we prepared crosslinked PTMA to prevent dissolution of the active material during cycling, which was confirmed using EQCM-D.[56]

Elsewhere, the charge storage mechanism has been investigated for a quinone polymer (poly[benzoquinonyl sulfide], PBQS) via a combination of EQCM-D and in situ Fourier transform infrared spectroscopy in a zinc electrolyte.[57] Because the Δf/n responses overlapped with each other and ΔD was close to zero, the authors analyzed Δf/n using the Sauerbrey equation. It was found that $Zn^{2+}$ was the transporting species in the PBQS polymer with no obvious hydration shell.

In addition, the swelling characteristics of conjugated conducting polymers have been evaluated using EQCM-D.[7,8,10,11,78,84] Cendra et al. conducted EQCM-D measurements of p(g2T-TT) in NaF, NaCl, and $NaBF_4$ aqueous electrolytes to reveal different swelling behaviors.[78] Whereas swelling the polymer with NaF (≈11%) and NaCl (≈13%) produced negligible mass uptake differences with respect to swelling with water (≈11%), contact with $NaBF_4$ almost doubled the mass (≈19%). Another work from Savva et al. quantified the amount of water incorporated into a p(g2T-TT) film and investigated structural and morphological changes occurring in the film upon electrochemical doping.[10] Together, these studies showed that solvent may be injected into the polymer film along with the ions during doping, but the nature of the anion,[78] electrolyte concentration,[10] and polymer structure[11] determine the swollen state of the polymer. This may in turn, impact morphology and crystal lattice spacings,[11] which govern electrical properties that are important for electrochemical devices.

In the field of biomedical applications, EQCM-D has been used to assess the adsorption of proteins in the absence and presence of applied electric potential on thin films.[85–87] The Pelton group evaluated polyvinylamine-g-TEMPO (PVAm-T)/laccase aging by monitoring the properties of adsorbed layers on a gold sulfonate sensor surface by QCM-D.[86] They found that there was a large decrease in both the magnitude of the frequency shift and the dissipation over the first 2 h of aging. This unusual aging property had influence on the redox properties of PVAm-T/laccase complexes. Cyclic voltammetry was used to measure the quantity of redox-active TEMPO in PVAm-T/laccase complexes adsorbed on the gold sulfonate sensor surfaces. The results showed that redox-activity of the PVAm-T/laccase decreased dramatically in the time that the complexes were aged before deposition. The quantity of adsorbed PVAm-T/laccase complex decreased with aging, giving a lower redox response. The authors also determined the influence of the TEMPO content in PVAm-T on the fraction of redox-active TEMPO in relatively well-defined LbL assemblies (PVAm-T) with sodium polystyrenesulfonate).[87]

Silva et al. investigated the adsorption dynamics of fibronectin (FN) driven by electrical stimulation on poly (3,4-ethylenedioxythiphene) copolymerized with poly(D,L-lactic acid)(PEDOT-*co*-PDLLA) thin films.[85] The effect of electrical stimulation on serum proteins was assessed using EQCM-D, and the authors found that, without electrical stimulation, the surfaces of both PEDOT-*co*-PDLLA and EDOT-PDLLA presented a similar amount of adsorbed FN. When an electrical potential was applied, a significantly larger amount of FN was adsorbed on both the Au interface and PEDOT-*co*-PDLLA, especially when an oxidized surface (positive potential) was employed.

Besides cyclic voltammetry, other electrochemical methods can be combined with QCM-D, including galvanostatic charge–discharge (GCD).[57] The experimental procedure and data analysis proceed similarly as to that described for cyclic voltammetry, except a constant current is applied for GCD. Oxidation and reduction charge is computed by integrating the current with respect to the charging or discarging time, respectively. For example, Zhang et. al. explored the charge storage mechanism for a quinone-based polymer electrode in a 3 M $Zn(OTf)_2$ in aqueous electrolyte using this technique in which the mass was quantified using a Sauerbrey model.[57] The charge stoarge mechanism involved transport of both cations and anions for charge neutralization except for the first discharge step in GCD cycle. Figure 9 (A) shows the voltage and mass change profile for the quinone polymer electrode during the first discharge step, where the mass change curve coincides with the theoritical Δm/Q of $Zn^{2+}$, reflecting the absence of anions or solvent from the prestine polymer electrode and charge being solely compensenated by $Zn^{2+}$. During the charging step, there was insertion of $OTf^-$ along with release of $Zn^{2+}$ resulting in an overall mass increase of the electrode. Figure 9(B) shows EQCM-D with CV during the first cycle where $F_{Faraday}$ coincides with the Δf/n curve in the negative scan and the deviation in the positive scan is due to the insertion of $OTf^-$ anions along with release of $Zn^{2+}$. Figure 9(C) shows the charge–discharge curve for the first two cycles of the quinone-based polymer, where an additional plateau around 1.1 V versus $Zn/Zn^{2+}$ shows the additional p-doping process. This confirms the co-participation of anions and cations in the electrode reaction.

## 4.3 | Measuring swelling to determine Flory-Huggins interaction parameters

The degree to which a polymer swells in a given solvent is related to polymer-solvent interactions, as described by

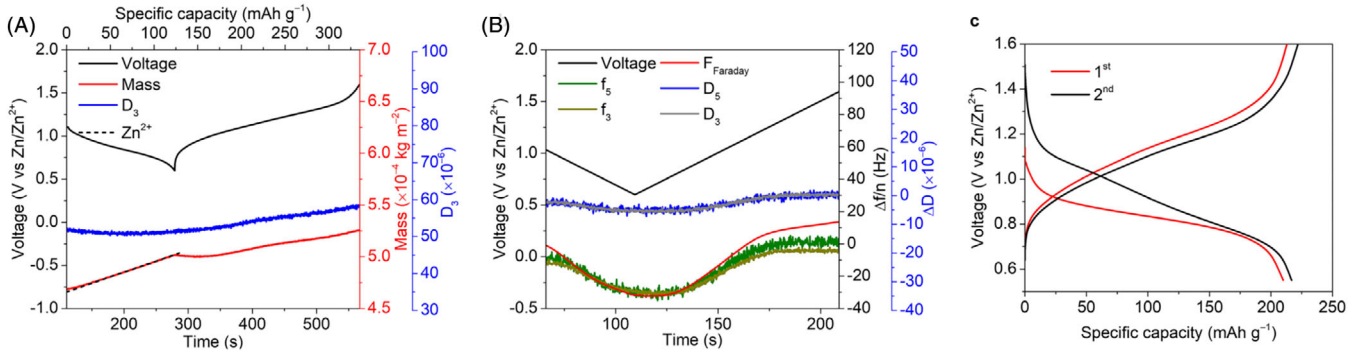


**FIGURE 9** (A) Change in mass, third overtone dissipation, and voltage along with time in the first galvanostatic charge–discharge cycle. (B) Voltage and EQCM-D response (third and fifth overtones) with time in the first CV cycle in a three-electrode configuration with quinone polymer as the working electrode, and zinc as the reference and counter electrode. (C) First and second galvanostatic charge–discharge cycles of a coin cell at the current density of 400 mAg$^{-1}$. The electrolyte was 3 M $Zn(OTf)_2$ in deionized water. Adapted from ref. 57 licensed under CC BY 4.0, IOPscience

Flory-Huggins theory.[9,88] QCM-D is ideal for monitoring the swelling of thin films because it allows for control over temperature and external environment. Here, we highlight one specific case that uses QCM-D to monitor swelling, which resulted in the determination of polymer-solvent Flory-Huggins interaction parameters. The Vogt group quantified the swelling of three model battery electrode binders (poly(vinylidene fluoride) (PVDF), PAA, and branched poly(ethylenimine) (BPEI) in common carbonate-based battery electrolytes to examine the volume fraction of carbonate in the swollen polymer film.[9]

PVDF was swollen to equilibrium in propylene carbonate (PC), from which the swollen thickness was determined using a viscoelastic model. Assuming that the swelling in the thin film was unidirectional, the swelling ratio of the swollen PVDF thin film was considered equivalent to the solvent volume fraction. The volume fraction of PC in the PVDF ($\phi_{PC}$) and of PVDF ($\phi_{PVDF}$) was then used to calculate the interaction parameter between the two, $\chi_{PC\text{-}PVDF}$, with Flory-Huggins theory using the following equation:

$$\ln(a_{PC}) = \ln(1-\phi_{PVDF}) + \phi_{PVDF} + \chi_{PVDF-PC} \times \phi_{PVDF}^2, \quad (8)$$

where $a_{PC}$ is the activity of PC. In this case for the pure PC, $a_{PC} = 1$, and the activity of PC in the solution is equal to its activity in the PVDF phase. The chemical potentials of the swollen polymer and solvent phase were assumed to be equal in order to obtain $\chi_{PVDF-PC}$.

Lastly, the authors found that the swelling of PVDF increased with increasing temperature and decreased slightly with addition of lithium salt. The ratio of ethylene carbonate and PC in the electrolyte impacted the binder's swelling more significantly than the selected lithium salt. The swelling and mechanical properties of polymer binders in aqueous and nonaqueous electrolyte has also been examined by others using EQCM-D.[49,51]

The Aurbach group used EQCM-D to demonstrate a strain-accommodation mechanism in high-strain $NaFePO_4$/PVDF electrodes via the relaxation of the binder network surrounding the intercalation particles.[51] The authors quantified the high-frequency viscoelastic properties of the high-strain composite electrodes correlated with their low-frequency resilience and toughness moduli. Fast relaxation ensured effective high-strain accommodation by the softened binder in aprotic solution. In contrast, with excessively stiff binder in aqueous solution, the strong electrode/binder interactions tracked dynamically to reflect the initial and advanced stages of the mechanical degradation of the polymeric binder up to its complete destruction. The discovered correlation between the fracture toughness of the binder and its high-frequency viscoelastic behavior will serve for a rational design of high-strain electrodes.

## 4.4 | Gas sensing

There is a growing interest in the detection of gasses, such as volatile organic compounds (VOCs) that are harmful to human health. In particular, VOCs have a low-molecular weight, exist in a gaseous state at room temperature, and their limited affinity for solid surfaces makes sensing very difficult. QCM-D is a technology suitable for gas sensing by monitoring changes in mass (due to gas sorption), and so far, many groups have detected VOCs via QCM-D monitoring of polymer films.

As shown in Figure 10(A), when VOC gas molecules are adsorbed onto the polymer-coated-QCM-D sensor, the mass of the polymer increases. As a result, the adsorption of VOC gas molecules manifests as a decrease in frequency as exemplified by the QCM-D frequency response shown in Figure 10(B). Su et al. adopted a

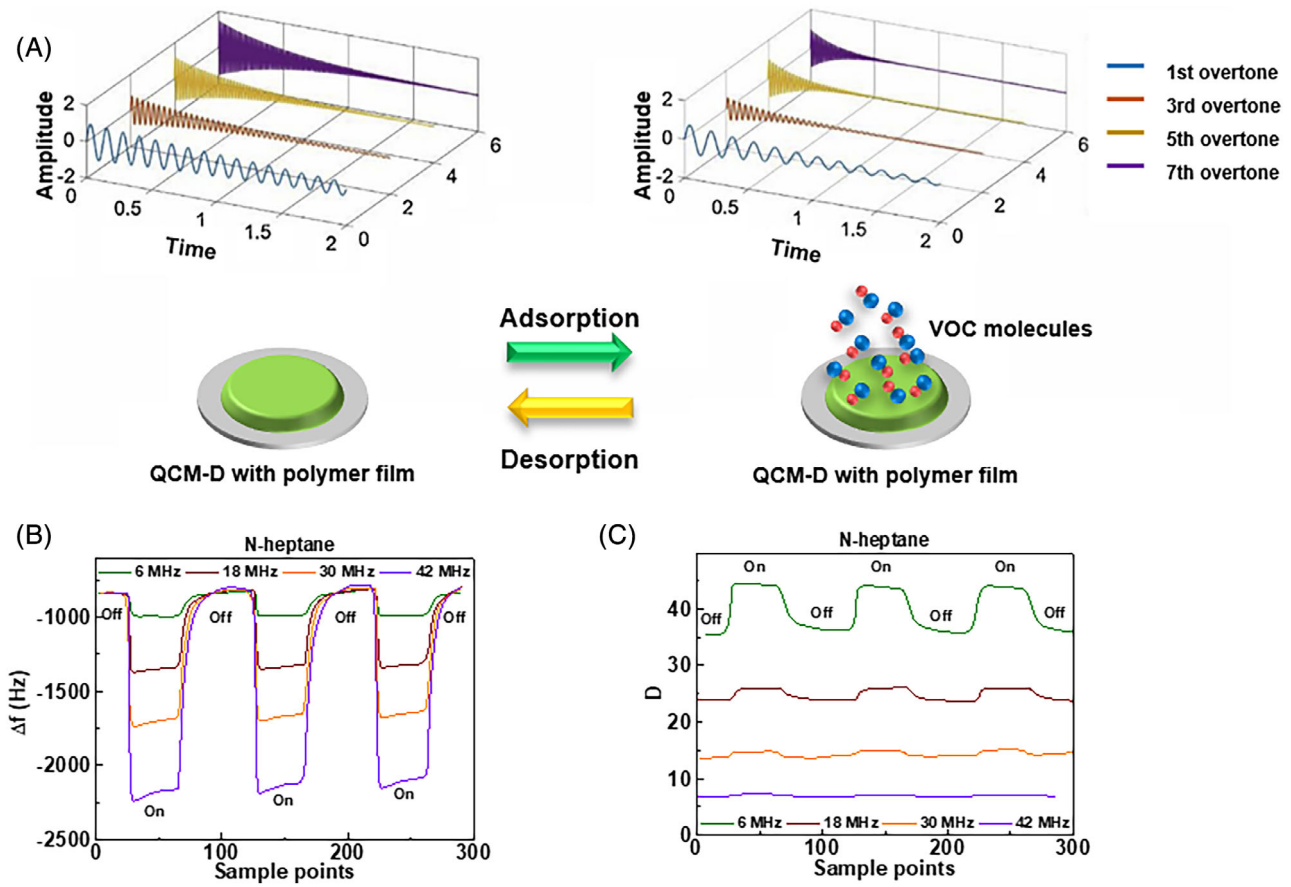


FIGURE 10 (A) Schematic diagram of the polymer-coated QCM-D sensor. Hypothetical QCM-D responses to VOC adsorption for four harmonics (1st, 3rd, 5th, and 7th) are shown. The (B) frequency and (C) dissipation responses for 6, 18, 30, and 42 MHz harmonics of the PVP-coated QCM-D sensor to a 50% saturated concentration of N-heptane repeated over three cycles. Reproduced with permission[89] copyright 2020, Wiley. PVP, polyvinylpyrrolidone; VOC, volatile organic compounds

wireless electrodeless (WE) QCM-D sensor with a multiple-resonance mode to identify VOCs, and employed polyvinylpyrrolidone (PVP) as the sensitive film to detect a variety of VOCs.[89] The frequency and energy dissipation of WE-QCM-D are shown in Figure 10 (B),(C). As shown in Figure 10(B), the resonance frequency shifts more at higher overtones, which is consistent with the Sauerbrey model. According to the Sauerbrey model, the frequency shift is linearly proportional to the vibrating frequency, and better sensitivity can be obtained at higher operating frequency. In Figure 10(C), energy dissipation decreases as the resonant frequency increases. In this study, the effect of the interaction between VOC molecules and PVP films on the viscoelastic properties of the polymer was identified.

## 4.5 | Protein adhesion and conformations

Previously, QCM-D has been widely applied to study the time-dependent adsorption and conformation of proteins onto polymer coatings and surfaces.[35,90,91] The affinity of the protein to the polymer coating is used to understand the coating's potential in biomedical applications, such as for medical implants and drug delivery. One notable challenge is that the amino acids that make up proteins typically have both hydrophilic and hydrophobic domains, which makes the surface hydrophobicity of a material an important consideration. If the wrong domain of the protein interacts with the material's surface, then the protein's binding sites may be hidden, thus making the protein inactive. Therefore, both the surface adsorption and binding orientation of the proteins should be considered when evaluating possible materials.

In one case study, QCM-D was applied to study the adsorption and conformation of fibrinogen (Fg), fibronectin (Fn), and bovine serum albumin (BSA) onto a variety of copolyesters based on butylene succinate (PBS) and dilinoleic succinate (DLS).[92] The proteins Fg and Fn are critical in wound healing. PBS:DLS copolymers were deposited onto Au-coated QCM sensors via spin-casting. After determining the dry film thickness, the authors swelled the polymer films with buffer solution. Finally,

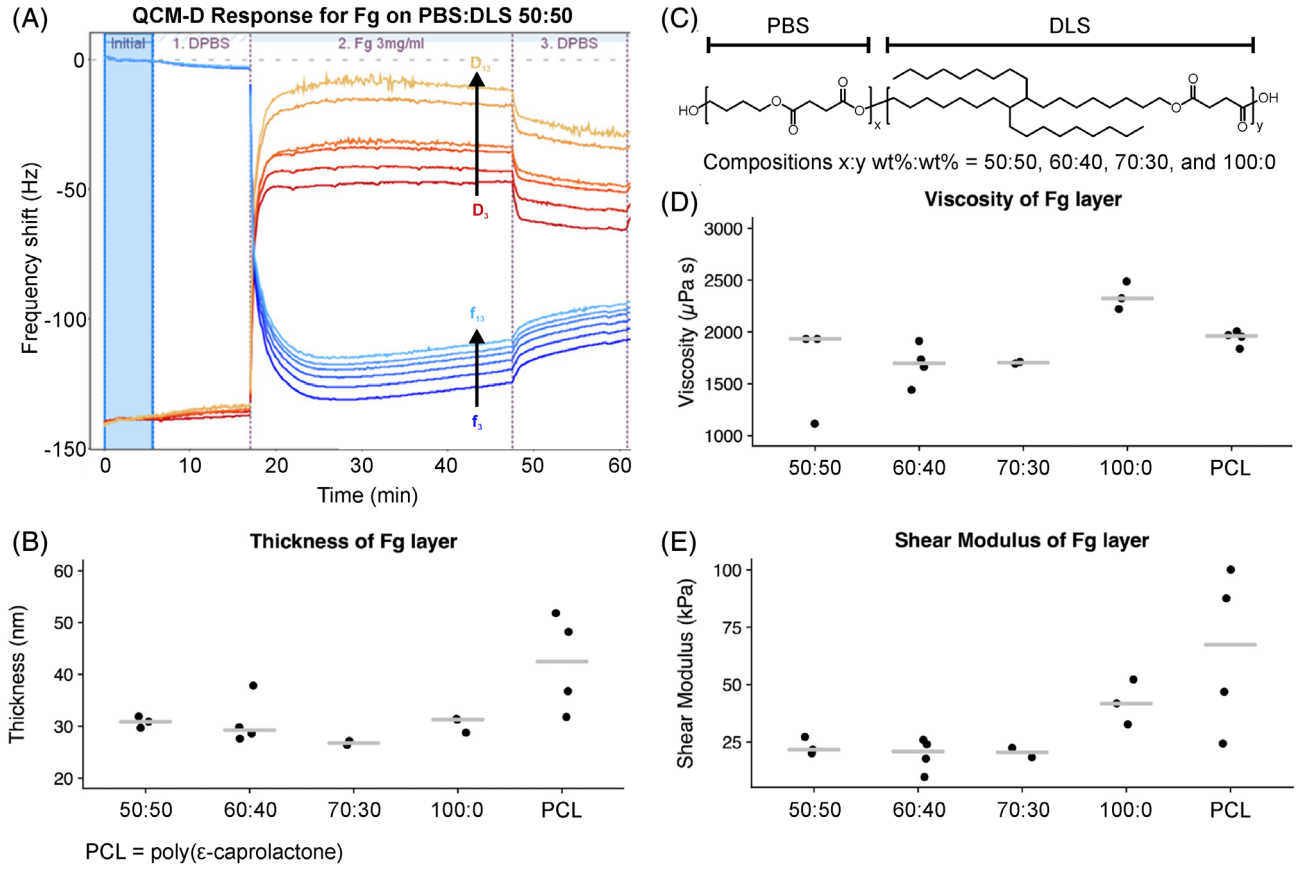


**FIGURE 11** (A) The QCM-D response of a 50:50 PBS:DLS copolymer when sequentially exposed to (1) Dulbecco's phosphate-buffered saline (DPBS), (2) Fg solution, and (3) DPBS. (B) The thickness of the absorbed Fg layer from fitting the Voigt viscoelastic model to the data. (C) The chemical structure of the copolymers considered. (D and E) The resulting viscosity and shear modulus, respectively, of the adsorbed Fg layer. Adapted with permission from ref. 92. Copyright the American Chemical Society 2019. DLS, dilinoleic succinate; PBS, butylene succinate

the sensors were exposed to the protein of interest (Fg, Fn, or BSA) using a flow cell, and the binding was evaluated by estimating the mass change. The orientation of the adsorbed proteins was evaluated by comparing the resulting thickness, viscosity, and shear modulus of the adsorbed layer from application of the Voigt viscoelastic model. Finally, the displacement of adhered proteins by additional exposure to a different protein was considered. Figure 11(A) shows the QCM-D response during this process, in which frequency decreases and dissipation increases as proteins form a thin layer on the PBS:DLS surface. Rinsing with buffer solution resulted in a slight increase in frequency as loosely bound Fg was washed away. A Voigt viscoelastic model was fit to the data from Figure 11(A), which resulted in estimates of the thickness, viscosity, and shear modulus of the adsorbed Fg layer. From Figure 11(B), the thickness of the Fg layer was ca. 30 nm for the copolyester surface and ca. 45 nm for a control PCL surface. Due to the large size of hydrated Fg (ca. 48 nm long cylinder), the authors concluded that this thickness change, coupled with the rapid kinetics of adsorption, suggested that the Fg proteins are bound in a tilted end-on orientation. This was further confirmed by viscosity values (Figure 11(D)) that were consistent with previous literature for highly hydrated Fg. Finally, the shear modulus (Figure 11(E)) for the copolyesters was lower than that of the control, suggesting that the adsorbed Fg on the copolymers were more hydrated. The authors concluded that the QCM-D data and fitted Fg layer parameters confirmed that the Fg was not in a side-on orientation, which is typically associated with denatured Fg. For materials in cell-contacting soft tissue applications, low-shear moduli and thick adsorption layers are preferred for increased cellular adhesion.[93] The results of this work, coupled with previous cellular proliferation studies of the polyesters,[94] suggest that polymers without biofunctionality exhibit high-protein adhesion when the shear modulus is similar to that of extracellular matrix.[92]

## 5 | CONCLUSION

This review examined the application of QCM-D to understand physical phenomena in polymer thin films. Special attention was devoted to practical operation of the instrument for new or entry-level users. QCM-D has captured widespread interest due to the technique's ability to sensitively measure changes in mass in real time and in a variety of environmental conditions. However, the sensitivity of the technique can create challenges for new users. For example, we examined the challenges of finding an appropriate film thickness, film deconstruction, bubble formation, and instrumental drift, as well as their remedies. The applications of QCM-D to specific cases (LbL assembly, electrochemistry, polymer swelling, gas sensing, and biomacromolecules) were presented.

Looking to the future, rapid growth is expected largely in the area of electrochemical QCM-D to analyze mixed electron-ion transfer for applications in organic electrochemical transistors and energy storage. This information will be valuable if coupled to measurements of electronic and ionic conductivity in order to fully understand the polymer's electrical and electrochemical behavior.

Although QCM-D saw some of its first applications to LbL assembly, there is still more room to explore. More advanced QCM-D modules allow for coupled measurements of the surface via (e.g.) ellipsometry or other methods. Together, these aspects will lend new information to understanding LbL films beyond just analyzing their growth behavior.

Another area of growth is gas sensing. Although not widely applied yet, QCM-D may prove useful for sensitively detecting mass changes due to gas sorption. However, it is our own personal experience that—at low levels of detector gas (ppb)—instrumental drift begins to compete with the response signal. This may be addressed by using polymer materials with stronger responses or thicker films.

In commentary to the community, we encourage researchers to include their modeling parameters in their reporting so that others can understand the validity of the chosen model. Further, researchers should disclose their baselining protocols so that others may understand how the relative frequency/dissipation changes were assessed. Lastly, with the technique being so sensitive and prone to the aforementioned challenges, researchers should reproduce their results many times, while also reporting so.

In closing, QCM-D offers unprecedented access to physical changes in polymer films that allows for a deeper understanding of film growth, film responses, mixed ion transport, solvent-polymer interactions, gas-polymer interactions, and molecular conformation. The technique is and will continue to be a powerful tool for the polymer community, especially in the areas of LbL assembly, redox polymers, and sensors.

## ACKNOWLEDGMENTS

This work was supported in part by grant DE-SC0014006 funded by the US Department of Energy, Office of Science (EQCM-D) and the National Science Foundation under Grant No. 1905732 (LbL QCM-D). A.D.E. acknowledges support by the National Science Foundation Graduate Research Fellowship under Grant No. DGE:1746932.

## DATA AVAILABILITY STATEMENT

Data sharing not applicable to this article as no new data were created during the current study.

## ORCID

*Jodie L. Lutkenhaus* https://orcid.org/0000-0002-2613-6016

## REFERENCES

[1] M. Rodahl, B. Kasemo, *Sens. Actuators, A* **1996**, *54*(1), 448.
[2] C. K. O'Sullivan, G. G. Guilbault, *Biosens. Bioelectron.* **1999**, *14*(8), 663.
[3] K. Keiji Kanazawa, J. G. Gordon, *Anal. Chim. Acta* **1985**, *175*, 99.
[4] G. Rudolph, A. Hermansson, A.-S. Jönsson, F. Lipnizki, *Sep. Purif. Technol.* **2021**, *254*, 117578.
[5] B. Cheng, K. Ishihara, H. Ejima, *Polym. Chem.* **2020**, *11*(2), 249.
[6] X. Ai, L. Mei, C. Ma, G. Zhang, *Prog. Org. Coat.* **2021**, *153*, 106141.
[7] J. L. Antonio, L. Höfler, T. Lindfors, S. I. Córdoba de Torresi, *ChemElectroChem* **2016**, *3*(12), 2146.
[8] M. Moser, T. C. Hidalgo, J. Surgailis, J. Gladisch, S. Ghosh, R. Sheelamanthula, Q. Thiburce, A. Giovannitti, A. Salleo, N. Gasparini, A. Wadsworth, I. Zozoulenko, M. Berggren, E. Stavrinidou, S. Inal, I. McCulloch, *Adv. Mater.* **2020**, *32*(37), e2002748.
[9] J. Qian, C. G. Wiener, Y. Zhu, B. D. Vogt, *Polymer* **2018**, *143*, 237.
[10] A. Savva, C. Cendra, A. Giugni, B. Torre, J. Surgailis, D. Ohayon, A. Giovannitti, I. McCulloch, E. Di Fabrizio, A. Salleo, J. Rivnay, S. Inal, *Chem. Mater.* **2019**, *31*(3), 927.
[11] P. Schmode, A. Savva, R. Kahl, D. Ohayon, F. Meichsner, O. Dolynchuk, T. Thurn-Albrecht, S. Inal, M. Thelakkat, *ACS Appl. Mater. Interfaces* **2020**, *12*(11), 13029.
[12] E. Guzmán, H. Ritacco, J. E. F. Rubio, R. G. Rubio, F. Ortega, *Soft Matter* **2009**, *5*(10), 2130.
[13] N. Parveen, P. K. Jana, M. Schönhoff, *Polymers* **2019**, *11*(8), 1285.
[14] J. T. O'Neal, E. Y. Dai, Y. Zhang, K. B. Clark, K. G. Wilcox, I. M. George, N. E. Ramasamy, D. Enriquez, P. Batys, M. Sammalkorpi, J. L. Lutkenhaus, *Langmuir* **2018**, *34*(3), 999.
[15] D. K. Reid, A. Summers, J. O'Neal, A. V. Kavarthapu, J. L. Lutkenhaus, *Macromolecules* **2016**, *49*(16), 5921.
[16] Q-Sense, in *Q-Sense E4 Operator Manual* (Ed: H. Uddenberg), Q-Sense AB, Sweden **2009**, p. 60.

[17] N. Shpigel, M. D. Levi, D. Aurbach, *Energy Storage Mater.* **2019**, *21*, 399.

[18] Q. Chen, S. Xu, Q. Liu, J. Masliyah, Z. Xu, *Adv. Colloid Interface Sci.* **2016**, *233*, 94.

[19] C. Tonda-Turo, I. Carmagnola, G. Ciardelli, *Front Bioeng. Biotechnol.* **2018**, *6*, 158.

[20] D. A. Buttry, M. D. Ward, *Chem. Rev.* **1992**, *92*(6), 1355.

[21] F. R. Lack, G. W. Willard, I. E. Fair, *Bell Syst. Tech. J.* **1934**, *13* (3), 453.

[22] K. Singh, C. F. Blanford, *ChemCatChem* **2014**, *6*(4), 921.

[23] A. Mirmohseni, V. Hassanzadeh, *J. Appl. Polym. Sci.* **2001**, *79* (6), 1062.

[24] J. L. Jordan, E. J. Fernandez, *Biotechnol. Bioeng.* **2008**, *101*(4), 837.

[25] T. E. Alexander, L. D. Lozeau, T. A. Camesano, *Cell Surface* **2019**, *5*, 100024.

[26] M. Rodahl, F. Höök, C. Fredriksson, C. A. Keller, A. Krozer, P. Brzezinski, M. Voinova, B. Kasemo, *Faraday Discuss.* **1997**, *107*(0), 229.

[27] M. V. Voinova, M. Rodahl, M. Jonson, B. Kasemo, *Phys. Scr.* **1999**, *59*(5), 391.

[28] M. D. Levi, N. Shpigel, S. Sigalov, V. Dargel, L. Daikhin, D. Aurbach, *Electrochim. Acta* **2017**, *232*, 271.

[29] N. C. Speller, N. Siraj, B. P. Regmi, H. Marzoughi, C. Neal, I. M. Warner, *Anal. Chem.* **2015**, *87*(10), 5156.

[30] N. Shpigel, M. D. Levi, S. Sigalov, L. Daikhin, D. Aurbach, *Acc. Chem. Res.* **2018**, *51*(1), 69.

[31] I. Reviakine, D. Johannsmann, R. P. Richter, *Anal. Chem.* **2011**, *83*(23), 8838.

[32] R. van der Westen, P. K. Sharma, H. De Raedt, I. Vermue, H. C. van der Mei, H. J. Busscher, *Phys. Chem. Chem. Phys.* **2017**, *19*(37), 25391.

[33] G. Sauerbrey, *Z. Phys.* **1959**, *155*(2), 206.

[34] S. Wang, F. Li, A. D. Easley, J. L. Lutkenhaus, *Nat. Mater.* **2019**, *18*(1), 69.

[35] P. Hampitak, D. Melendrez, M. Iliut, M. Fresquet, N. Parsons, B. Spencer, T. A. Jowitt, A. Vijayaraghavan, *Carbon* **2020**, *165*, 317.

[36] B. D. Vogt, E. K. Lin, W.-L. Wu, C. C. White, *J. Phys. Chem. B* **2004**, *108*(34), 12685.

[37] N.-J. Cho, C. W. Frank, B. Kasemo, F. Höök, *Nat. Protoc.* **2010**, *5*(6), 1096.

[38] M. Rodahl, B. Kasemo, *Rev. Sci. Instrum.* **1996**, *67*(9), 3238.

[39] S. M. S. Schönwälder, F. Bally, L. Heinke, C. Azucena, Ö. D. Bulut, S. Heißler, F. Kirschhöfer, T. P. Gebauer, A. T. Neffe, A. Lendlein, G. Brenner-Weiß, J. Lahann, A. Welle, J. Overhage, C. Wöll, *Biomacromolecules* **2014**, *15*(7), 2398.

[40] W. Wang, Y. Xu, S. Backes, A. Li, S. Micciulla, A. B. Kayitmazer, L. Li, X. Guo, R. von Klitzing, *Langmuir* **2016**, *32*(14), 3365.

[41] Scientific, B, How to read a QCM specification.

[42] Taguchi, N.; Maebayashi, M.; Koda, S. Evaluation of Viscoelasticity of Polymer Films in High-Temperature Region by a QCM-D Method. Presented at: Proc. of Symp. on Ultrasonic Electronics, **2010**; pp 297–298.

[43] E. F. Irwin, J. E. Ho, S. R. Kane, K. E. Healy, *Langmuir* **2005**, *21*(12), 5529.

[44] N. B. Eisele, F. I. Andersson, S. Frey, R. P. Richter, *Biomacromolecules* **2012**, *13*(8), 2322.

[45] K. Sadman, C. G. Wiener, R. A. Weiss, C. C. White, K. R. Shull, B. D. Vogt, *Anal. Chem.* **2018**, *90*(6), 4079.

[46] F. Höök, B. Kasemo, T. Nylander, C. Fant, K. Sott, H. Elwing, *Anal. Chem.* **2001**, *73*(24), 5796.

[47] D. Johannsmann, *The Quartz Crystal Microbalance in Soft Matter Research*, 1st ed., Springer, Cham, Switzerland **2015**.

[48] J. J. J. Gillissen, S. R. Tabaei, J. A. Jackman, N.-J. Cho, *Analyst* **2017**, *142*(18), 3370.

[49] N. Jäckel, V. Dargel, N. Shpigel, S. Sigalov, M. D. Levi, L. Daikhin, D. Aurbach, V. Presser, *J. Power Sources* **2017**, *371*, 162.

[50] Z. Adamczyk, M. Sadowska, P. Żeliszewska, *Anal. Chem.* **2020**, *92*(22), 15087.

[51] N. Shpigel, S. Sigalov, M. D. Levi, T. Mathis, L. Daikhin, A. Janes, E. Lust, Y. Gogotsi, D. Aurbach, *Joule* **2018**, *2*(5), 988.

[52] D. Johannsmann, *Phys. Chem. Chem. Phys.* **2008**, *10*(31), 4516.

[53] QSense, *Cleaning & Immobilization Protocols.*, Gothenburg, Sweden: Q-Sense AB; **2008**.

[54] E. S. Muckley, L. Collins, B. R. Srijanto, I. N. Ivanov, *Adv. Funct. Mater.* **2020**, *30*(10), 1908010.

[55] K. M. Persson, R. Gabrielsson, A. Sawatdee, D. Nilsson, P. Konradsson, M. Berggren, *Langmuir* **2014**, *30*(21), 6257.

[56] S. Wang, A. M. G. Park, P. Flouda, A. D. Easley, F. Li, T. Ma, G. D. Fuchs, J. L. Lutkenhaus, *ChemSusChem* **2020**, *13*(9), 2371.

[57] Y. Zhang, Y. Liang, H. Dong, X. Wang, Y. Yao, *J. Electrochem. Soc.* **2020**, *167*(7), 070558.

[58] J. L. S. Antonio, V. L. Martins, S. I. Córdoba de Torresi, R. M. Torresi, *Electrochim. Acta* **2019**, *324*, 134887.

[59] G. Decher, J. D. Hong, J. Schmitt, *Thin Solid Films* **1992**, *210-211*, 831.

[60] G. Decher, *Science* **1997**, *277*(5330), 1232.

[61] A. Vidyasagar, C. Sung, K. Losensky, J. L. Lutkenhaus, *Macromolecules* **2012**, *45*(22), 9169.

[62] A. Vidyasagar, C. Sung, R. Gamble, J. L. Lutkenhaus, *ACS Nano* **2012**, *6*(7), 6174.

[63] Scientific, B QCM-D Measurement. https://www.biolinscientific.com/measurements/qcm-d.

[64] J. D. Torrey, T. L. Kirschling, L. F. Greenlee, *J. Res. Natl. Inst. Stand. Technol.* **2015**, *120*, 1.

[65] A. Savva, S. Wustoni, S. Inal, *J. Mater. Chem. C* **2018**, *6*(44), 12023.

[66] A. Rao, S. Kang, B. D. Vogt, V. M. Prabhu, E. K. Lin, W.-L. Wu, M. Muthukumar, *Langmuir* **2006**, *22*(24), 10009.

[67] M. Koenig, T. Kasputis, D. Schmidt, K. B. Rodenhausen, K.-J. Eichhorn, A. K. Pannier, M. Schubert, M. Stamm, P. Uhlmann, *Anal. Bioanal. Chem.* **2014**, *406*(28), 7233.

[68] P. Handa, C. Fant, M. Nydén, *Prog. Org. Coat.* **2006**, *57*(4), 376.

[69] T. K. Lind, M. W. A. Skoda, M. Cárdenas, *ACS Omega* **2019**, *4* (6), 10687.

[70] G. Ohlsson, P. Axelsson, J. Henry, S. Petronis, S. Svedhem, B. Kasemo, *Microfluid. Nanofluid.* **2010**, *9*(4), 705.

[71] N. L. Benbow, J. L. Webber, P. Pawliszak, D. A. Sebben, S. Karpiniec, D. Stringer, M. J. Tobin, J. Vongsvivut, M. Krasowska, D. A. Beattie, *J. Colloid Interface Sci.* **2019**, *553*, 720.

[72] A. vander Straeten, C. Dupont-Gillain, *ACS Appl. Polym. Mater.* **2020**, *2*(7), 2602.

[73] A. vander Straeten, A. Bratek-Skicki, A. M. Jonas, C.-A. Fustin, C. Dupont-Gillain, *ACS Nano* **2018**, *12*(8), 8372.

[74] A. vander Straeten, A. Bratek-Skicki, L. Germain, C. D'Haese, P. Eloy, C. A. Fustin, C. Dupont-Gillain, *Nanoscale* **2017**, *9*(44), 17186.

[75] P. G. Kitz, M. J. Lacey, P. Novak, E. J. Berg, *Anal. Chem.* **2019**, *91*(3), 2296.

[76] N. Mozhzhukhina, E. Flores, R. Lundstrom, V. Nystrom, P. G. Kitz, K. Edstrom, E. J. Berg, *J. Phys. Chem. Lett.* **2020**, *11*(10), 4119.

[77] N. Shpigel, M. D. Levi, X. Cheng, T. Cao, R. Wu, T. S. Mathis, Y. Zhang, D. Aurbach, Y. Gogotsi, *ACS Energy Lett.* **2019**, *4*(8), 1907.

[78] C. Cendra, A. Giovannitti, A. Savva, V. Venkatraman, I. McCulloch, A. Salleo, S. Inal, J. Rivnay, *Adv. Funct. Mater.* **2019**, *29*(5).
[79] Y. Zhang, Q. Zeng, Y. Shen, L. Yang, F. Yu, *ACS Appl. Mater. Interfaces* **2020**, *12*(50), 56216.
[80] V. V. Shumyantseva, T. V. Bulko, L. V. Sigolaeva, A. V. Kuzikov, A. I. Archakov, *Biosens. Bioelectron.* **2016**, *86*, 330.
[81] J. G. Wu, S. C. Wei, S. C. Luo, *Adv. Mater. Interfaces* **2020**, *7*(15).
[82] N. Elgrishi, K. J. Rountree, B. D. McCarthy, E. S. Rountree, T. T. Eisenhart, J. L. Dempsey, *J. Chem. Educ.* **2017**, *95*(2), 197.
[83] F. Scholz, *Electroanalytical Methods*, Springer, Berlin **2002**.
[84] A. Savva, D. Ohayon, J. Surgailis, A. F. Paterson, T. C. Hidalgo, X. Chen, I. P. Maria, B. D. Paulsen, A. J. Petty, J. Rivnay, I. McCulloch, S. Inal, *Adv. Electron. Mater.* **2019**, *5*(8).
[85] A. C. da Silva, R. A. da Silva, M. Souza, P. M. Montoya, R. Bentini, T. Augusto, R. M. Torresi, L. H. Catalani, S. I. Cordoba de Torresi, *Biointerphases* **2020**, *15*(2), 21003.
[86] Q. Fu, A. Sutherland, E. Gustafsson, M. M. Ali, L. Soleymani, R. Pelton, *Langmuir: ACS J. Surfaces Colloids* **2017**, *33*(32), 7854.
[87] Q. Fu, I. Zoudanov, E. Gustafsson, D. Yang, L. Soleymani, R. H. Pelton, *ACS Appl. Mater. Interfaces* **2017**, *9*(6), 5622.
[88] A. D. Easley, L. M. Vukin, P. Flouda, D. L. Howard, J. L. Pena, J. L. Lutkenhaus, *Macromolecules* **2020**, *53*, 7997.
[89] X. Su, D. Chen, N. Li, A. C. Stevenson, G. Li, R. Hu, *Sens. Actuators, A* **2020**, *305*, 111938.
[90] M. Tagaya, *Polym. J.* **2015**, *47*(9), 599.
[91] K. A. Marx, *Biomacromolecules* **2003**, *4*(5), 1099.
[92] P. Sobolewski, N. S. Murthy, J. Kohn, M. El Fray, *Langmuir* **2019**, *35*(26), 8850.
[93] D. E. Discher, P. Janmey, Y. L. Wang, *Science* **2005**, *310*(5751), 1139.
[94] S. Agueda, S. Rahul, S. Karolina, B. Julia, W. Aleksandra, M. Andrew, S. Peter, S. XiaoMeng, E. P. Judit, K. Joachim, W. H. Daniel, E. F. Miroslawa, *Mater. Sci. Eng. C Mater. Biol. Appl.* **2019**, *108*.

## AUTHOR BIOGRAPHIES

**Alexandra D. Easley** is currently a PhD candidate in the Materials Science and Engineering Department at Texas A&M University and is currently working with Prof. Jodie Lutkenhaus. Her research interests include redox active polymers, solution conformations, and interactions of these polymers, and their applications in fully polymeric batteries.

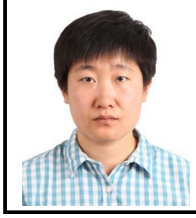

**Ting Ma** currently works as a postdoctoral researcher in the group of Prof. Jodie Lutkenhaus at Texas A&M University. She obtained her PhD under the supervision of Prof. Jun Chen from Nankai University. Her current research interest focuses on polymer-based metal-free aqueous batteries.

**Chikaodinaka I. Eneh** is currently a Chemical Engineering PhD student working for Prof. Jodie Lutkenhaus at Texas A&M University. Her research focuses on the phase transition and hydration of polyelectrolyte complexes and multilayers as a response to changes in assembly and post-assembly conditions.

**Junyeong Yun** is currently a postdoctoral researcher under Prof. Jodie Lutkenhaus at the Department of Chemical Engineering. He received his PhD degree in Chemical and Biological Engineering from Korea University. His research interests include 2D transition metal carbides (MXenes) and organic radical polymers, as well as their applications in supercapacitors and batteries for energy storage.

**Ratul Mitra Thakur** is currently a Chemical Engineering PhD student and is currently working with Prof. Jodie Lutkenhaus. His research interests include redox active polymers, doping mechanism of these polymers and their applications in energy storage devices.

**Jodie Lutkenhaus** is the Axalta Chair and Professor in the Artie McFerrin Department of Chemical Engineering at Texas A&M University. She is recognized for her expertise in the thermal behavior and water effects of polyelectrolyte complexes, redox mechanisms in polymer electrodes, and composites for high-stiffness batteries.

**How to cite this article:** A. D. Easley, T. Ma, C. I. Eneh, J. Yun, R. M. Thakur, J. L. Lutkenhaus, *J Polym Sci* **2021**, 1. https://doi.org/10.1002/pol.20210324